International Journal of Control and Automation
Vol.7, No.10 (2014), pp.217-232
http://dx.doi.org/10.14257/ijca.2014.7.10.20

Direct Torque Control of PMSM Based on Fractional Order Sliding Mode Variable Structure and Experiment Research

Jiacai Huang, Lei Cui and Xinxin Shi

Automation School, Nanjing Institute of Technology, Nanjing 211167, China
huangjiacai@126.com

Abstract

A direct torque control method based on fractional order sliding mode variable structure (DTC-FOSMVS) was proposed for the speed control of a permanent magnet synchronous motor (PMSM). The proposed method in which the space vector pulse width modulation (SVPWM) with fixed switch frequency is applied, reduces the torque and flux ripple, and improves the speed control performance. In order to improve the energy efficiency and reduce the demagnetization effect, the DTC-FOSMVS method with dynamic flux reference was designed. The stability of the control method is proved by Lyapunov theory. The performance of the proposed method is verified through experiment which is based on hardware in loop and Simulink/QuaRC real time control software. The experiment results show the robustness and effectiveness of the proposed method.

Keywords: *Fractional calculus; Fractional order sliding mode variable structure; Permanent magnet synchronous motor; Direct torque control; Dynamic flux reference*

1. Introduction

Due to the superior features such as compact structure, high efficiency, high torque to inertia ratio, and high power density [1], the permanent magnet synchronous motor (PMSM) has many applications in industries. In order to obtain excellent dynamic performance, many interests are focused on the control algorithm of the PMSM. The most famous two control methods of PMSM are the field oriented control (FOC) method [2-4] and direct torque control (DTC) method [5-16]. Although the two methods are widely studied and used in application, the DTC method has many advantages over FOC method such as low parameter dependence, fast dynamic response, and simple configuration. Because of these advantages, the DTC method has been received great attention.

The DTC method was first applied for the induction motor by Depenbrock and Takahashi In 1980's [5,6]. In the late 1990s, the DTC technique was used in the permanent magnet synchronous motor [7,8]. In the conventional DTC system where the hysteresis controllers are used, the flux and torque ripple exist, and the switching frequency is variable. All of these drawbacks of DTC make it unusable in some special applications. In order to improve the classical DTC performances, a modified DTC algorithm with fixed switching frequency for PMSM was proposed to reduce the flux and torque ripples [9-11]. In [12], a modified DTC algorithm which can reduce both torque and flux linkage ripples has been proposed for an IPMSM without speed sensor. In [13], the modified DTC algorithm which is based on PI regulator and space vector modulation (SVM) has been proposed. In industrial application, the parameter variation and load disturbance are inevitable, in order to improve the robustness of the DTC system, the sliding mode variable structure control was adopted into the DTC algorithm [14-16]. In the conventional sliding mode based DTC methods, the sliding mode

ISSN: 2005-4297 IJCA

surfaced is usually designed with the integer order calculus of the state variables.

Fractional calculus has a 300 years old history, and for a long time, it was considered as a pure theoretical subject with nearly no applications. But, in recent decades the application of fractional controller attracts increasing attention due to the more degree of freedom that provided [17-22].

This article applies the fractional calculus into the DTC system, and proposes a kind of modified DTC algorithm which is based on fractional order sliding mode variable structure and space vector pulse width modulation. The proposed method reduces the torque and flux ripple, improves the speed control performance. The experiment results demonstrate the effectiveness of the proposed method.

The rest of this paper is organized as follows. In Section 2, the fractional order calculus operation is introduced. In Section 3, the mathematical model of PMSM is introduced. In Section 4 the direct torque control algorithm based on fractional order sliding mode variable structure (DTC-FOSMVS) with constant flux reference was proposed. In Section 5, the DTC-FOSMVS method with dynamic flux reference was proposed. In section 6, the stability of the control system is proved. In Section 7, the effectiveness of the proposed algorithm is illustrated through real time experiment and compared with the conventional DTC method. Finally, conclusions are presented in Section 8.

2. Fractional Calculus

Fractional calculus is a generalization of integer order integration and differentiation to non-integer order ones. Let symbol ${}_aD_t^\lambda$ denotes the fractional order fundamental operator, defined as follows [20]:

$$ {}_aD_t^\lambda \square D^\lambda = \begin{cases} \dfrac{d^\lambda}{dt^\lambda} & R(\lambda) > 0 \\ 1 & R(\lambda) = 0 \\ \int_a^t (d\tau)^{-\lambda} & R(\lambda) < 0 \end{cases} \tag{1} $$

Where a and t are the time limits of the operation, λ is the order of the operation, and generally $\lambda \in R$ and λ can be a complex number.

The three most used definitions for the general fractional differentiation and integration are the Grunwald-Letnikov(GL) definition, the Riemann-Liouville(RL) definition and the Caputo definition [21, 22].

(a). The GL definition is given as

$$ {}_aD_t^\lambda f(t) = \lim_{h \to 0} h^{-\lambda} \sum_{j=0}^{\left[\frac{t-a}{h}\right]} (-1)^j \binom{\lambda}{j} f(t - jh) \tag{2} $$

where λ is the arbitrarily order, $[\cdot]$ means the integer part, h denotes the calculation step length, $\binom{\lambda}{j}$ is the binomial coefficient, and

$$ \binom{\lambda}{j} = \frac{\lambda!}{j!(\lambda - j)!} = \frac{\Gamma(\lambda + 1)}{\Gamma(j+1)\Gamma(\lambda - j + 1)} \tag{3} $$

where $\Gamma(\cdot)$ is the *Gamma* function, defined as

$$\Gamma(x) = \int_0^{+\infty} e^{-t} t^{x-1} dt \tag{4}$$

(b). The RL definition is given as

$${}_a D_t^{\lambda} f(t) = \frac{1}{\Gamma(n-\lambda)} \frac{d^n}{dt^n} \int_a^t \frac{f(\tau)}{(t-\tau)^{\lambda-n+1}} d\tau \tag{5}$$

where $n-1 < \lambda < n$.

(c). The Caputo definition is given as

$${}_a D_t^{\lambda} f(t) = \frac{1}{\Gamma(n-\lambda)} \int_a^t \frac{f^n(\tau)}{(t-\tau)^{\lambda-n+1}} d\tau \tag{6}$$

where $n-1 < \lambda < n$.

Having zero initial conditions, the Laplace transformation of the RL definition for a fractional order λ is given by

$$L\left\{ {}_a D_t^{\lambda} f(t) \right\} = s^{\lambda} F(s) \tag{7}$$

Where $F(s)$ is *Laplace* transformation of $f(t)$. Distinctly, the fractional-order operator has more degrees of freedom than that with integer order.

3. Mathematical Model of PMSM

The PMSM is composed of a stator and a rotor, the rotor is made by a permanent magnet, and the stator has 3-phase windings which are distributed sinusoidally. The voltage equations for a PMSM in the rotor d-q reference frame are given as [24]:

$$\begin{bmatrix} u_d \\ u_q \end{bmatrix} = \begin{bmatrix} R + pL_d & -\omega_e L_q \\ \omega_e L_d & R + pL_q \end{bmatrix} \begin{bmatrix} i_d \\ i_q \end{bmatrix} + \begin{bmatrix} 0 \\ \omega_e \psi_f \end{bmatrix} \tag{8}$$

where u_d and u_q are voltages in the d- and q- axes, i_d and i_q are currents in the d- and q- axes, L_d and L_q are inductances in the d- and q- axes, R is the stator resistance, ω_e is electrical angular velocity, ψ_f is the flux linkage of the permanent magnet, p denotes the differential operator.

Through the following coordinate transformation [23]:

$$\begin{bmatrix} f_d \\ f_q \end{bmatrix} = \begin{bmatrix} \cos\theta_e & \sin\theta_e \\ -\sin\theta_e & \cos\theta_e \end{bmatrix} \begin{bmatrix} f_\alpha \\ f_\beta \end{bmatrix} \tag{9}$$

the mathematics model for a PMSM in the stationary α-β reference frame can be expressed as:

$$\begin{bmatrix} u_\alpha \\ u_\beta \end{bmatrix} = \begin{bmatrix} R + pL_d & \omega_e (L_d - L_q) \\ -\omega_e (L_d - L_q) & R + pL_d \end{bmatrix} \begin{bmatrix} i_\alpha \\ i_\beta \end{bmatrix} + \left\{ (L_d - L_q)(\omega_e i_d - \frac{\mathrm{d}i_q}{\mathrm{d}t}) + \omega_e \psi_f \right\} \begin{bmatrix} -\sin\theta_e \\ \cos\theta_e \end{bmatrix} \tag{10}$$

where f_α and f_β are the variables in the α-β stationary reference frame, f_d and f_q are the variables in the d-q rotor reference frame. u_α and u_β are the voltages in the α-β stationary

reference frame, θ_e is the rotor position angle between the stationary reference frame and the rotor reference frame.

Define the back-EMF e_α and e_β as follows:

$$\begin{bmatrix} e_\alpha \\ e_\beta \end{bmatrix} = \left\{ (L_d - L_q)(\omega_e i_d - \frac{\mathrm{d}i_q}{\mathrm{d}t}) + \omega_e \psi_f \right\} \begin{bmatrix} -\sin\theta_e \\ \cos\theta_e \end{bmatrix} \tag{11}$$

then Eq.(10) can be rewritten as the following state equation:

$$\begin{bmatrix} \frac{\mathrm{d}i_\alpha}{\mathrm{d}t} \\ \frac{\mathrm{d}i_\beta}{\mathrm{d}t} \end{bmatrix} = \begin{bmatrix} -\frac{R}{L_d} & -\frac{\omega_e(L_d - L_q)}{L_d} \\ \frac{\omega_e(L_d - L_q)}{L_d} & -\frac{R}{L_d} \end{bmatrix} \begin{bmatrix} i_\alpha \\ i_\beta \end{bmatrix} - \begin{bmatrix} \frac{1}{L_d} & 0 \\ 0 & \frac{1}{L_d} \end{bmatrix} \begin{bmatrix} e_\alpha \\ e_\beta \end{bmatrix} + \frac{1}{L_d} \begin{bmatrix} u_\alpha \\ u_\beta \end{bmatrix} \tag{12}$$

The stator flux linkage in the α-β stationary reference frame can be expressed as

$$\begin{cases} \frac{\mathrm{d}\psi_\alpha}{\mathrm{d}t} = u_\alpha - R i_\alpha \\ \frac{\mathrm{d}\psi_\beta}{\mathrm{d}t} = u_\beta - R i_\beta \end{cases} \tag{13}$$

and the electromagnetic torque is estimated as

$$T = 1.5P\left(\psi_\alpha i_\beta - \psi_\beta i_\alpha\right) \tag{14}$$

where T is the electromagnetic torque, and P is the pole number of the rotor.

The square of the flux linkage is estimated as

$$\psi = \psi_\alpha^2 + \psi_\beta^2 \tag{15}$$

4. Direct Torque Control Based on Fractional Order Sliding Mode Variable Structure (DTC-FOSMVS) with Constant Flux Reference

The design of the sliding mode variable structure control mainly contains two steps, the first step is to select the sliding surface, which is usually the linear or nonlinear manifold of the state variables; the second step is to determine the control input, which drives the system state to the designed sliding surface and constrains the state to the surface subsequently.

In this DTC control method, the fractional order sliding surface for the flux linkage and direct torque are defined as follows:

$$S = \begin{bmatrix} S_T \\ S_\psi \end{bmatrix} = \begin{bmatrix} e_T + c_1 \cdot {}_0D_t^{-u} e_T \\ e_\psi + c_1 \cdot {}_0D_t^{-u} e_\psi \end{bmatrix} = \begin{bmatrix} e_T + c_1 D^{-u} e_T \\ e_\psi + c_1 D^{-u} e_\psi \end{bmatrix} \tag{16}$$

where $e_T = T^* - T$, $e_\psi = \psi^* - \psi$, and T^* is the reference torque, ψ^* is the flux reference. c_1 is the coefficient of the sliding surface and $c_1 \in R^+$. The symbol $D^{-u} = {}_0D_t^{-u}$ denotes the fractional order fundamental operator defined as Eq.(1), where u is called the order of the sliding surface and $0 < u < 1$.

Here the exponential reaching law is applied, and one can get

$$\dot{S} = \begin{bmatrix} \dot{S}_T \\ \dot{S}_\psi \end{bmatrix} = \begin{bmatrix} \dot{e}_T + c_1 D^{1-u} e_T \\ \dot{e}_\psi + c_1 D^{1-u} e_\psi \end{bmatrix} = \begin{bmatrix} -K_T S_T - \varepsilon_T \operatorname{sgn}(S_T) \\ -K_\psi S_\psi - \varepsilon_\psi \operatorname{sgn}(S_\psi) \end{bmatrix} \tag{17}$$

where $\operatorname{sgn}(x)$ denotes the sign function defined as:

$$\operatorname{sgn}(x) = \begin{cases} 1 & x > 0 \\ 0 & x = 0 \\ -1 & x < 0 \end{cases} \tag{18}$$

Taking the time derivative on both sides of (16) yields

$$\dot{S} = \begin{bmatrix} \dot{S}_T \\ \dot{S}_\psi \end{bmatrix} = \begin{bmatrix} \dot{e}_T + c_1 D^{1-u} e_T \\ \dot{e}_\psi + c_1 D^{1-u} e_\psi \end{bmatrix} = \begin{bmatrix} -\dot{T} + c_1 D^{1-u} e_T \\ -\dot{\psi} + c_1 D^{1-u} e_\psi \end{bmatrix} \tag{19}$$

4.1. Calculation of $\dot{S}_T$

From (14), the derivative of T can be obtained as

$$\dot{T} = 1.5P\left\{(i_\beta - \frac{\psi_\beta}{L_d})u_\alpha + (\frac{\psi_\alpha}{L_d} - i_\alpha)u_\beta - \frac{\psi_\alpha(Ri_\beta + e_\beta)}{L_d} + \frac{\psi_\beta(Ri_\alpha + e_\alpha)}{L_d} + \frac{\omega_e(L_d - L_q)}{L_d}(\psi_\alpha i_\alpha + \psi_\beta i_\beta)\right\} \tag{20}$$

Substituting (20) into (19), we can get the derivative of S_T which is described as follows:

$$\dot{S}_T = -\dot{T} + c_1 D^{1-u} e_T = -1.5P(i_\beta - \frac{\psi_\beta}{L_d})u_\alpha - 1.5P(\frac{\psi_\alpha}{L_d} - i_\alpha)u_\beta + c_1 D^{1-u} e_T + A_1 \tag{21}$$

where

$$A_1 = -1.5P\left\{\frac{\omega_e(L_d - L_q)}{L_d}(\psi_\alpha i_\alpha + \psi_\beta i_\beta) - \frac{\psi_\alpha(Ri_\beta + e_\beta)}{L_d} + \frac{\psi_\beta(Ri_\alpha + e_\alpha)}{L_d}\right\} \tag{22}$$

4.2. Calculation of $\dot{S}_\psi$

From (15) we have

$$\dot{\psi} = 2\psi_\alpha\dot{\psi}_\alpha + 2\psi_\beta\dot{\psi}_\beta = 2\psi_\alpha u_\alpha + 2\psi_\beta u_\beta - 2\psi_\alpha Ri_\alpha - 2\psi_\beta Ri_\beta \tag{23}$$

Substituting (23) into (19), we can get the derivative of S_ψ which is described as follows:

$$\dot{S}_\psi = -\dot{\psi} + c_1 D^{1-u} e_\psi = -2\psi_\alpha u_\alpha - 2\psi_\beta u_\beta + c_1 D^{1-u} e_\psi + A_2 \tag{24}$$

Where

$$A_2 = 2\psi_\alpha Ri_\alpha + 2\psi_\beta Ri_\beta \tag{25}$$

With Eq.(17), (21) and (24), we have

$$\dot{S} = \begin{bmatrix} \dot{S}_T \\ \dot{S}_\psi \end{bmatrix} = A + F + BU = \begin{bmatrix} -K_T S_T - \varepsilon_T \operatorname{sgn}(S_T) \\ -K_\psi S_\psi - \varepsilon_\psi \operatorname{sgn}(S_\psi) \end{bmatrix} \tag{26}$$

where

$$B = \begin{bmatrix} -1.5P(i_\beta - \frac{\psi_\beta}{L_d}) & -1.5P(\frac{\psi_\alpha}{L_d} - i_\alpha) \\ -2\psi_\alpha & -2\psi_\beta \end{bmatrix} \tag{27}$$

$$A = \begin{bmatrix} A_1 \\ A_2 \end{bmatrix}, \quad U = \begin{bmatrix} u_\alpha \\ u_\beta \end{bmatrix}, \quad F = \begin{bmatrix} c_1 D^{1-u} e_T \\ c_1 D^{1-u} e_\psi \end{bmatrix} \tag{28}$$

When the system works in the sliding mode, we have $\dot{S} = 0$, so from (26), the control output can be obtain as

$$U = B^{-1}\left\{ -A - F + \begin{bmatrix} -K_T S_T - \varepsilon_T \operatorname{sgn}(S_T) \\ -K_\psi S_\psi - \varepsilon_\psi \operatorname{sgn}(S_\psi) \end{bmatrix} \right\} \tag{29}$$

Obviously, after the voltage u_α and u_β are obtained from Eq.(29), then the space vector pulse width modulation (SVPWM) control method can be applied to the control process. Figure 1 is the speed control system with the proposed DTC-FOSMVS method.

In order to reduce the system chattering, the saturation function which is defined as Eq.(30) is applied.

$$\operatorname{sgn}(x) = \begin{cases} 1 & x/\varepsilon > 1 \\ x/\varepsilon & |x/\varepsilon| < 1 \\ -1 & x/\varepsilon < -1 \end{cases} \tag{30}$$

where ε is a positive small value.

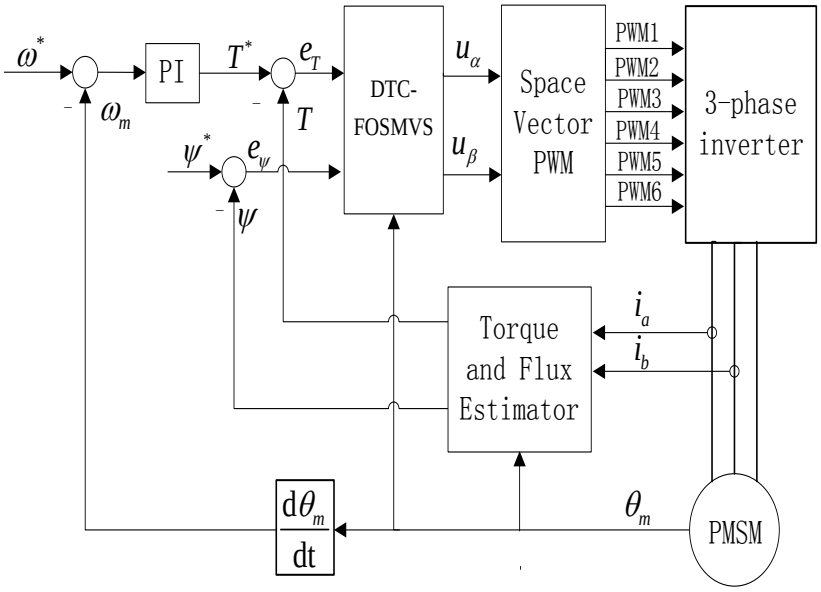

Figure 1. Block Diagram of the Proposed DTC-FOSMVS Control System with Constant Flux Reference

5. Direct Torque Control Based on Fractional Order Sliding Mode Variable Structure (DTC-FOSMVS) with Dynamic Flux Reference

In the above DTC control method, when the flux reference is constant, then the d-axis current i_d is not zero, which means that there exists nonzero demagnetization or magnetization component. The permanent magnet of the motor already supplies adequate magnetic field that needed for PMSM running, so the nonzero i_d is not only unnecessary, but also increases the energy consumption and reduces the system efficiency. In this section the minimization of i_d is considered in the proposed DTC-FOSMVS method.

In the rotor d-q reference frame, the flux equation is given as follow:

$$\begin{cases} \psi_d = L_d i_d + \psi_f \\ \psi_q = L_q i_q \end{cases} \tag{31}$$

Where ψ_d and ψ_q are the d-q components of the stator flux linkage.

The electromagnetic torque in d-q reference frame is estimated as

$$T = 1.5P(\psi_d i_q - \psi_q i_d) = 1.5P\psi_f i_q + 1.5P i_d i_q (L_d - L_q) \tag{32}$$

The square of the flux linkage is estimated as

$$\psi = \psi_d^2 + \psi_q^2 \tag{33}$$

From (32) and (33) it can be seen that for a constant flux reference ψ^*, when the system reaches at the steady state and moves on sliding surface, we have

$$T = T^* \Rightarrow 1.5P\psi_f i_q + 1.5P i_d i_q (L_d - L_q) = T^* \tag{34}$$

$$\psi = \psi^* \Rightarrow \psi_d^2 + \psi_q^2 = \psi^* \tag{35}$$

From the equation (34), i_q and can be obtained as

$$i_q = \frac{T^*}{1.5P\psi_f + 1.5P i_d (L_d - L_q)} \tag{36}$$

Substituting (36) into (31) and (35), i_d can be the solved from the following equation:

$$\left(L_d i_d + \psi_f\right)^2 + L_q^2 \left(\frac{T^*}{1.5P\psi_f + 1.5P i_d (L_d - L_q)} \right)^2 = \psi^* \tag{37}$$

It is clear that when

$$\psi^* = \psi_f^2 + \left(\frac{L_q T^*}{1.5P\psi_f} \right)^2 \tag{38}$$

then the d-axis current i_d will be zero as expected. When the load torque changes, the reference torque T^* will also change correspondingly, then from (38) it can be seen that the flux reference ψ^* will also change dynamically in order to maintain $i_d = 0$.

Figure 2 is the speed control system of the proposed DTC-FOSMVS method with dynamic flux reference.

6. Stability of the Control Method

The *Lyapunov* function is selected as

$$V = \frac{1}{2} S^T S \tag{39}$$

where S is defined as Eq.(16). The derivative of the *Lyapunov* function is

$$\dot{V} = S^T \dot{S} = S^T (A + F + BU) \tag{40}$$

Substituting Eq.(29) into Eq.(40) results in

$$\dot{V} = S^T \begin{bmatrix} -K_T S_T - \varepsilon_T \operatorname{sgn}(S_T) \\ -K_\psi S_\psi - \varepsilon_\psi \operatorname{sgn}(S_\psi) \end{bmatrix} = S_T \left(-K_T S_T - \varepsilon_T \operatorname{sgn}(S_T)\right) + S_\psi \left(-K_\psi S_\psi - \varepsilon_\psi \operatorname{sgn}(S_\psi)\right) \tag{41}$$

Because K_T and K_ψ are positive values, we have

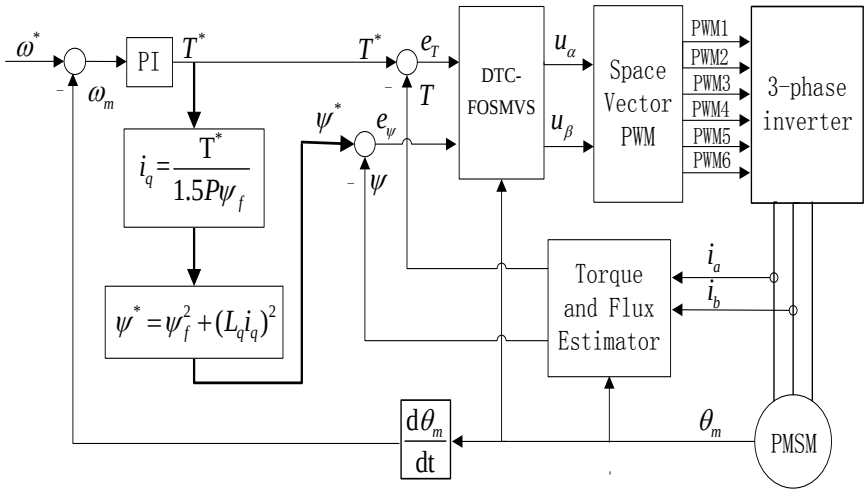

Figure 2. Block Diagram of the Proposed DTC-FOSMVS Control System With Dynamic Flux Reference

$$\begin{cases} S_T \left(-K_T S_T - \varepsilon_T \operatorname{sgn}(S_T)\right) < 0 \\ S_\psi \left(-K_\psi S_\psi - \varepsilon_\psi \operatorname{sgn}(S_\psi)\right) < 0 \end{cases} \tag{42}$$

From Eq.(41) and Eq.(42) it is obvious that $\dot{V} = S^T \dot{S} < 0$, so the system is globally stable, S and $\dot{S}$ will be forced to zero in a definite period, which also means that the torque and flux of the PMSM will follow their reference values respectively.

7. Experiment Research Based on Hardware in Loop and Simulink/ QuaRC

The effectiveness and robustness of the proposed control method is verified through the real time experiment platform which is based on hardware in loop and Simulink/QuaRC, as shown in Figure 3. The experiment platform contains a load PMSM, a tested PMSM, a torque

sensor, a driver board, and a computer in which a Simulink/QuaRC real time control software and a QPID data acquisition card are installed. In Figure 3, the load PMSM works under torque controlled mode, and generates different kind of load disturbance precisely. The torque sensor acquires the torque produced by the tested PMSM, and output the torque data to Simulink/QuaRC through QPID card. The proposed DTC-FOSMVS control method executes in the Simulink/QuaRC real time control software, and finally outputs the SVPWM control signals to the driver board through the QPID card.

In the experiment, the specifications of the tested PMSM are as follow: $R=0.985\Omega$, $P=4$, $\psi_f=0.081\mathrm{Wb}$, $L_d=2.96\mathrm{mH}$, $L_q=2.96\mathrm{mH}$, $J=0.425\times10^{-3}\mathrm{Kg\cdot m^2}$. The order of the sliding surface is $u=0.95$. The dynamic performance of the proposed method is tested and compared with the conventional DTC method and the DTC-SMC (direct torque control based on sliding mode controller) method.

Experiment 1: The dynamic performance of the proposed method with constant reference flux linkage is tested. The speed reference is $\omega^*=800$ r/min, the torque load is $1\mathrm{Nm}$, and the flux reference is $\psi^*=0.1$. Figure4-8 are the speed response, torque response, flux response, fractional order sliding surface S_ψ and S_T , respectively. From the experiment results it can be seen that the proposed method has small torque variation, and can reach and maintain at the reference speed.

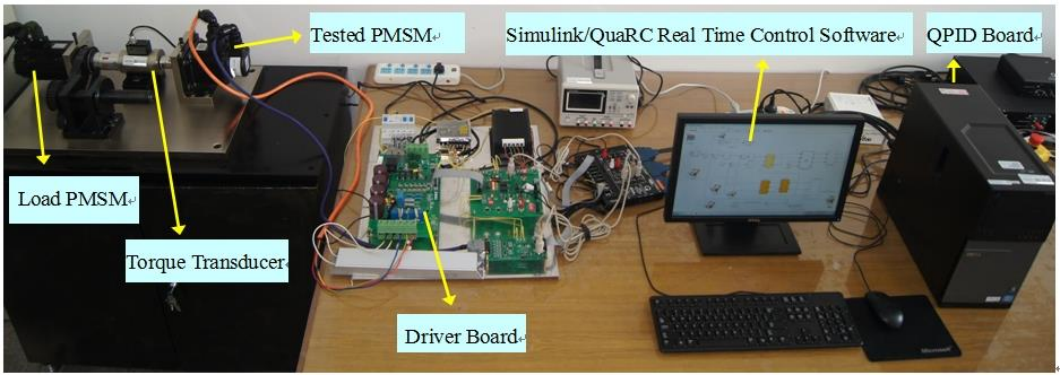

Figure 3. Real time experiment platform based on hardware in loop and Simulink/QuaRC

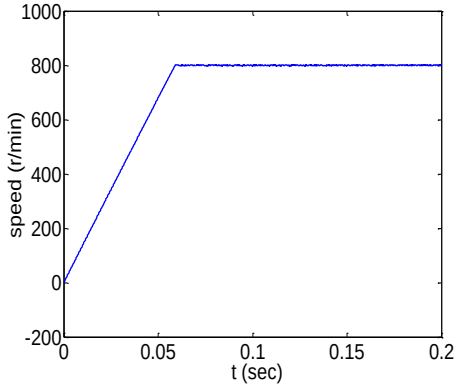

Figure 4. Speed Response

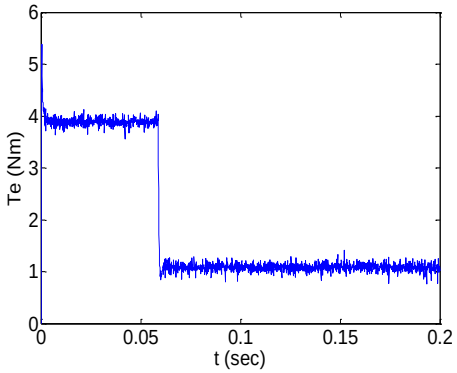

Figure 5. Torque Response

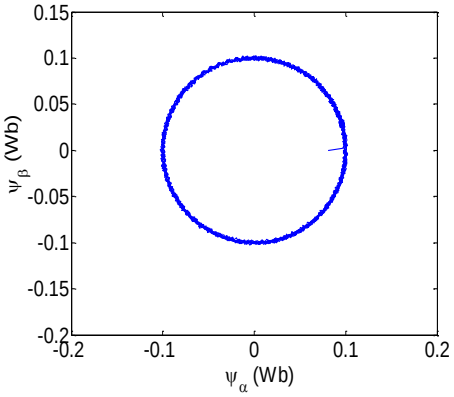

Figure 6. Flux Response

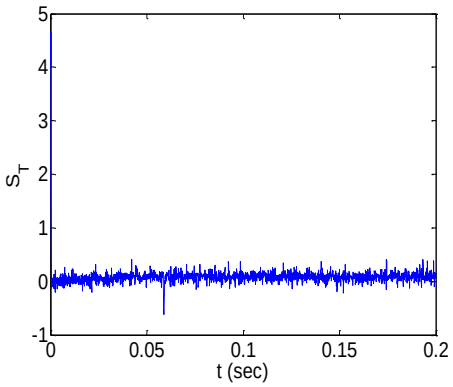

Figure 7. Sliding Surface S_T

Experiment 2: In this experiment, the dynamic performance under load disturbance of the proposed method is compared with that of the conventional DTC method. The flux reference ψ^* is constant and $\psi^* = 0.1$, the speed reference is $\omega^* = 800$ r/min. The load torque is $1\mathrm{N\,m}$, and a load disturbance of $1\mathrm{N\,m}$ appears at $t = 0.1s$.

Figure 9 and Figure 10 are the flux response and torque response of the proposed method and the conventional DTC method respectively. From the results it can be seen that when the load disturbance happens, both of the two methods can output torque to restrict the load disturbance, but the flux and torque fluctuation of the proposed method are smaller than those of the conventional DTC method.

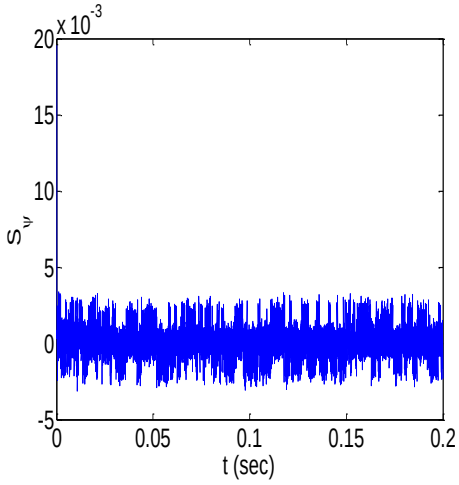

Figure 8. Sliding surface S_ψ

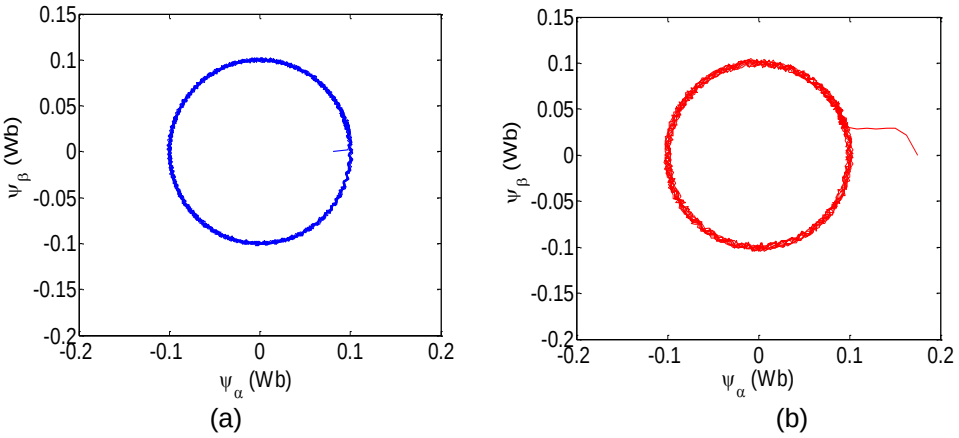

Figure 9. Flux response. (a) the proposed method, (b) the conventional DTC method

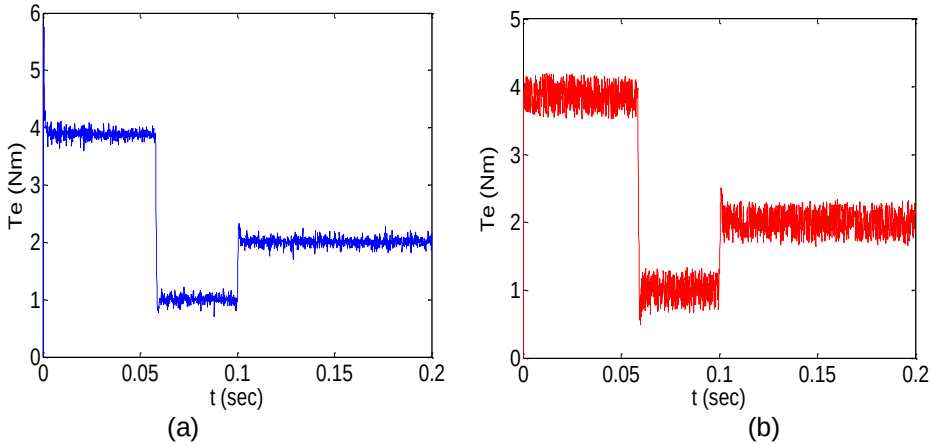

Figure 10. Torque Response. (a) the Proposed Method, (b) the Conventional DTC Method

Experiment 3: In this experiment, the dynamic performance under load disturbance of the proposed method is compared with that of the conventional DTC-SMC (direct torque control based on sliding mode controller) method. The load torque is $1\mathrm{N\,m}$, and a load disturbance of $1\mathrm{N\,m}$ appears at $t = 0.1s$ and vanishes at $t = 0.11s$.

Figure 11 and Figure 12 are the speed response and torque response of the proposed method and the conventional DTC-SMC method respectively. From the results it can be seen that both of the two methods have small torque fluctuation, but from Figure 11 (b) we can see that the speed response of the proposed method has smaller speed deviation than that of the conventional DTC-SMC method when the load disturbance happens.

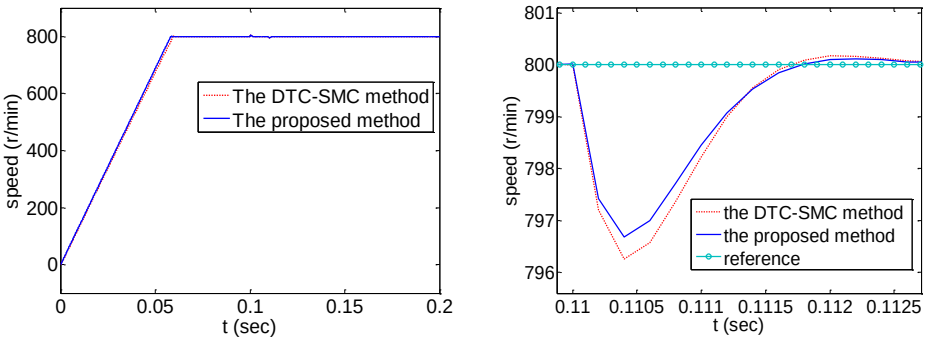

(a) Speed response (b) Partial enlarged detail of the speed response

Figure 11. Speed response of the proposed method and the conventional DTC-SMC method

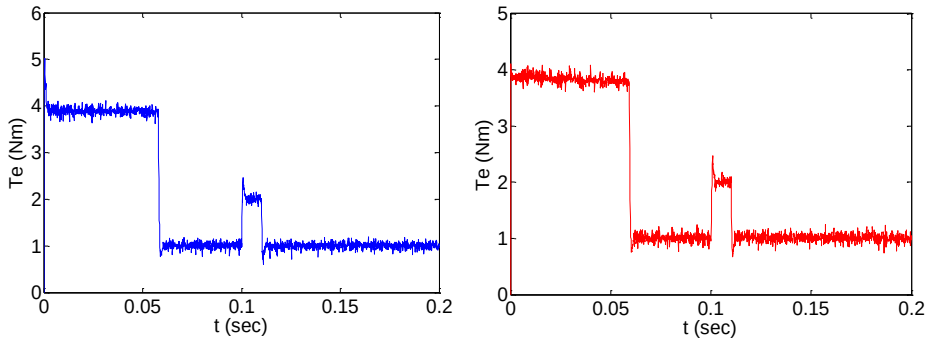

(a) (b)

Figure 12. Torque Response. (a) the Proposed Method, (b) the Conventional DTC-SMC Method

Experiment 4: In this experiment, the dynamic performance of the proposed method under constant flux reference mode and dynamic flux reference mode are tested and compared. The speed reference is $\omega^*=800$ r/min, the load torque is $1\mathrm{Nm}$. In the constant flux reference mode, we set $\psi^*=0.1$, as shown in Figure 13. In the dynamic flux reference mode, the flux reference ψ^* is dynamically calculated by the speed regulator, as shown in Figure 14. The responses of speed, i_q, i_d,and torque are shown as Figure 15-18.

Figure 14 shows that the flux reference ψ^* is changed dynamically in the speed control process. From Figure 17 it can be seen that the q-axis currents i_q in both modes are similar, meanwhile from Figure 16 it is obviously that in the constant flux reference mode the d-axis current i_d is not zero, while in the dynamic flux reference mode the i_d is near zero. This means that the energy efficiency in dynamic flux reference mode is higher than that in the constant flux reference mode, and moreover the demagnetization effect in the dynamic flux reference mode is reduced.

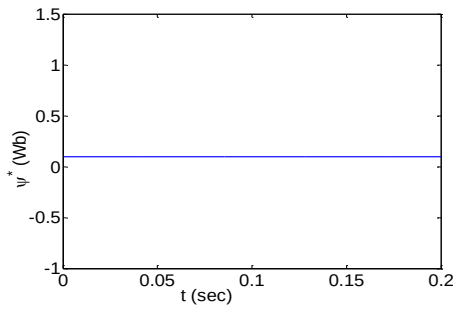

Figure 13. Constant Flux Reference

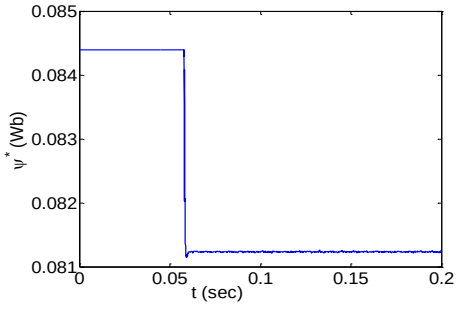

Figure 14. Dynamic Flux Reference

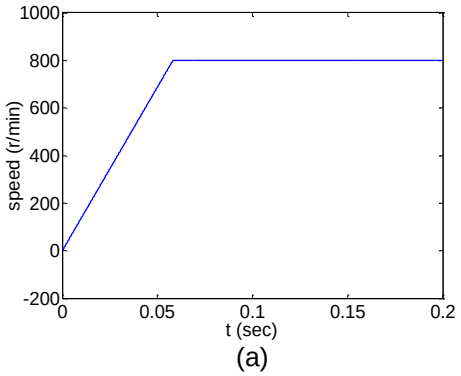

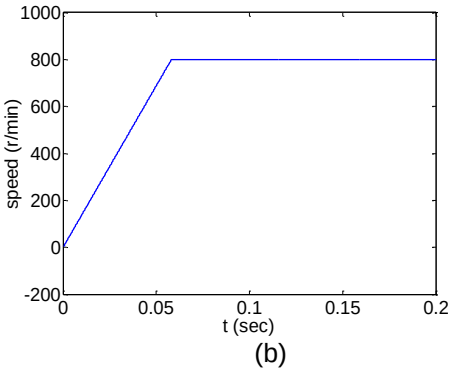

Figure 15. Speed Response. (a) with Constant Flux Reference, (b) with Dynamic Flux Reference

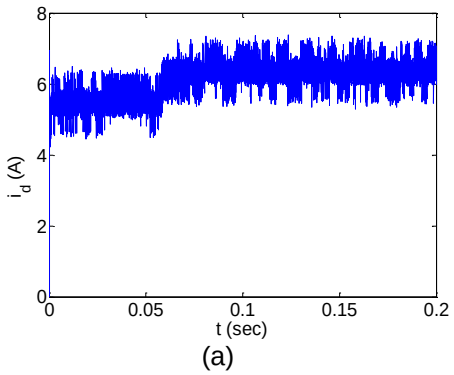

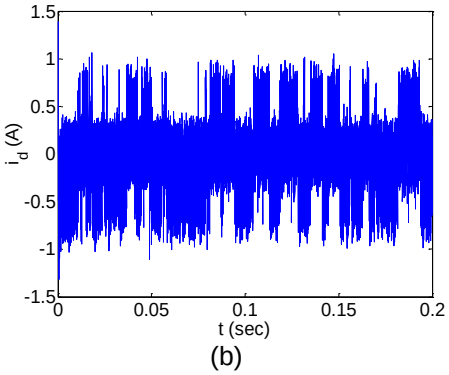

Figure 16. Current i_d Response. (a) With Constant Flux Reference, (b) With Dynamic Flux Reference

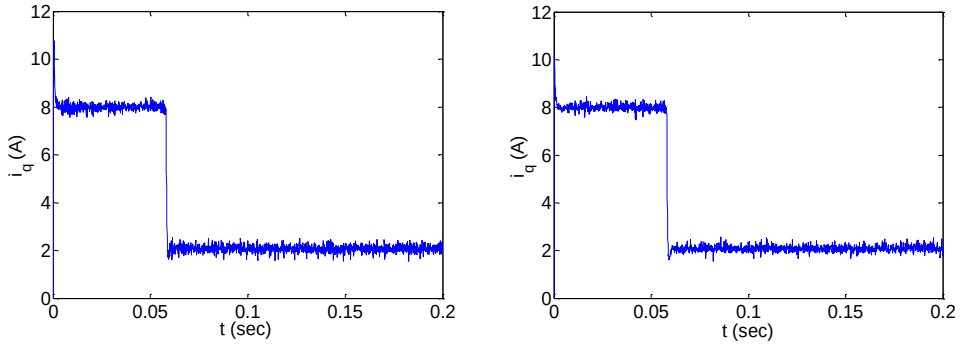

Figure 17. Current i_q Response. (a) With Constant Flux Reference, (b) With Dynamic Flux Reference

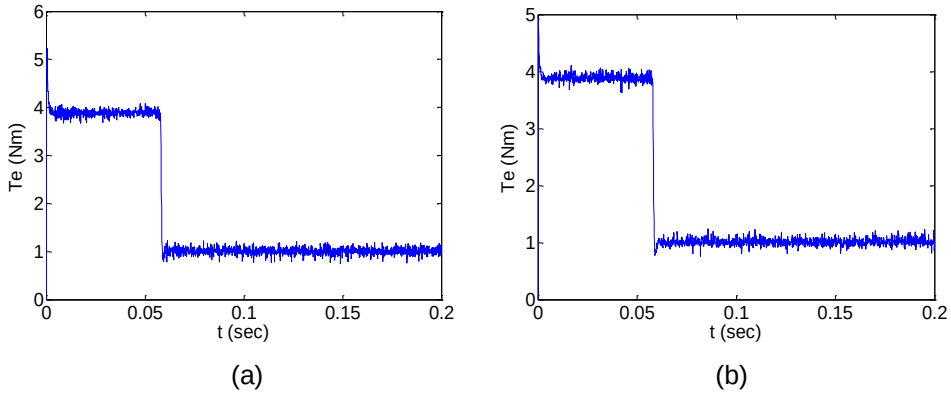

Figure 18. Torque Response. (a) With Constant Flux Feference, (b) With Dynamic Flux Reference

8. Conclusions

A kind of direct torque control method based on fractional order sliding mode variable structure (DTC-FOSMVS) was proposed for the speed control of the permanent magnet synchronous motor (PMSM). The proposed method can reduce the torque and flux ripple, and has small speed deviation when load disturbance happens. In order to improve the energy efficiency and reduce the demagnetization effect, the DTC-FOSMVS method with dynamic flux reference was also designed. The stability of the control method is proved by Lyapunov theory. The performance of the proposed method is verified through the experiment platform which is based on hardware in loop and Simulink/QuaRC real time control software. The experiment results show the effectiveness of the proposed method.

Acknowledgements

This work was supported by National Natural Science Foundation (NNSF) of China under Grant (61104085), the natural science foundation of Jiangsu Province (BK20130744), and the Jiangsu Government Scholarship for Overseas Studies(JS-2012-051).

References

[1] G. R. Slemon, "Electrical machines for variable-frequency drives", Proceeding of IEEE, vol. 82, no. 8, **(1994)**, pp. 1123-1139.
[2] C. K. Lai and K. K. Shyu, "A novel motor drive design for incremental motion system via sliding-mode control method", IEEE Transactions on Industrial Electronics, vol. 52, no. 2, **(2005)**, pp. 499-507.
[3] A. M. Harb, "Nonlinear chaos control in a permanent magnet reluctance machine", Chaos, Solitons & Fractals, vol. 19, no. 5, **(2004)**, pp. 1217-1224.
[4] J. Zhou and Y. Wang, "Real-time nonlinear adaptive back stepping speed control for a PM synchronous motor", Control Engineering Practice, vol. 13, no. 10, **(2005)**, pp. 1259-1269.
[5] M. Depenbrock, "Direct self-control of inverter-fed machine," IEEE Transactions on Power Electronics, vol. 3, no. 4, **(1988)**, pp. 420-429.
[6] I. Takahashi and T. Naguchi, "A new quick-response and high-efficiency control strategy of an induction motor," IEEE Transactions on Industry Applications, vol. 5, **(1986)**, pp. 820-827.
[7] C. French and P. Acarnley, "Direct torque control of permanent magnet drives," IEEE Transactions on Industry Applications, vol. 32, no. 5, **(1996)**, pp. 1080-1088.
[8] L. Zhong, M. F. Rahman, W. Y. Hu, and K. W. Lim, "Analysis of direct torque control in permanent magnet synchronous motor drives," IEEE Transactions on Power Electronics, vol. 12, no. 3, **(1997)**, pp. 528-536.
[9] L. Tang and M. F. Rahman, "A new direct torque control strategy for flux and torque ripple reduction for induction motors drive by using space vector modulation", Proceedings of IEEE 32nd Annual Conference on Power Electronics Specialists, vol. 3, **(2001)**, pp. 1440-1445.
[10] D. Swierczynski, M. Kazmierkowski and F. Blaabjerg, "DSP based direct torque control of permanent magnet synchronous motor (PMSM) using space vector modulation (DTC-SVM)", International Symposium on Industrial Electronics (ISIE). vol. 3, **(2002)**, pp. 723-727.
[11] K. Chikh, A. Saad, M. Khafallah and D. YousfiA, "Novel drive implementation for PMSM by using direct torque control with space vector modulation", Canadian Journal on Electrical and Electronics Engineering, vol. 2, no. 8, **(2011)**, pp. 400-408.
[12] L. Tang, L. Zhong, M. F. Rahman and Y. Hu, "A novel direct torque control for interior permanent magnet synchronous machine drive with low ripple in torque and flux-a speed-sensorless approach", IEEE Transactions on Industry Applications, vol. 39, no. 6, **(2003)**, pp. 1748-1756.
[13] M. S. Raj, T. Saravanan and V. Srinivasan, "A modified direct torque control of induction motor using space vector modulation technique", Middle-East Journal of Scientific Research, vol. 20, no. 11, **(2014)**, pp. 1572-1574.
[14] S. Z. Chen, N. C. Cheung, K. C. Wong and J. Wu, "Integral sliding-mode direct torque control of doubly-fed induction generators under unbalanced grid voltage", IEEE Transactions on Energy Conversion, vol. 25, no. 2, **(2010)**, pp. 356-368.
[15] A. Aimad, K. Madjid and S. Mekhilef, "Robust sensorless sliding mode flux observer for DTC-SVM-based drive with Inverter nonlinearity compensation", Journal of Power Electronics, vol. 14, no. 1, **(2014)**, pp. 125-134.
[16] K. T. Orlowska and G. Tarchala, "Integral sliding mode direct torque control of the induction motor drives", Proceedings of IEEE 39th Annual Conference on Industrial Electronics, **(2013)**, pp. 8482-8487.
[17] I. Podlubny, "Fractional-order systems and $PI^{\lambda}D^{\mu}$- controllers", IEEE Transactions on Automatic Control, vol. 44, no. 1, **(1999)**, pp. 208-214.
[18] H. S. Li, Y. Luo and Y. Q. Chen, "A fractional order proportional and derivative (FOPD) motion controller: tuning rule and experiments", IEEE Transactions on Control Systems Technology, vol. 18, no. 2, **(2010)**, pp. 516-520.
[19] Y. Li, Y.Q. Chen and I. Podlubny, "Stability of fractional order nonlinear dynamic systems: Lyapunov direct method and generalized Mittag-Leffler stability", Computers & Mathematics with Applications, vol. 59, no. 5, **(2010)**, pp. 1810-1821.
[20] Y. Q. Chen, I. Petras and D. Y. Xue, "Fractional order control-A tutorial", Proceedings of American Control Conference, **(2009)**, pp. 1397- 1411.
[21] K. B. Oldham and J. Spanier, "The fractional calculus", Academic Press, New York **(1974)**.
[22] I. Podlubny, "Fractional differential equations", Academic Press, San Diego **(1999)**.
[23] H. P. Jia and Y. K. He, "Variable structure sliding mode control for PMSM DTC", Transaction of china electro-technical society, vol. 21, no. 1, **(2006)**, pp.1-6.
[24] F. J. Lin, "Real-time IP position controller design with torque feedforward control for PM synchronous motor", IEEE Transactions on Industrial Electronics, vol. 44, no. 3, **(1997)**, pp. 398–407.

[25] F. Khoucha, K. Marouani, M. Benbouzid, A. Kheloui and A. Mamoune, "A 7-Level Single DC source cascaded H-Bridge multilevel inverter with a modified DTC scheme for induction motor-based electric vehicle propulsion", International Journal of Vehicular Technology, **(2013)**, pp. 1-9.

